

# Energy & Environmental Science

Accepted Manuscript



This is an *Accepted Manuscript*, which has been through the Royal Society of Chemistry peer review process and has been accepted for publication.

*Accepted Manuscripts* are published online shortly after acceptance, before technical editing, formatting and proof reading. Using this free service, authors can make their results available to the community, in citable form, before we publish the edited article. We will replace this *Accepted Manuscript* with the edited and formatted *Advance Article* as soon as it is available.

You can find more information about *Accepted Manuscripts* in the [Information for Authors](#).

Please note that technical editing may introduce minor changes to the text and/or graphics, which may alter content. The journal's standard [Terms & Conditions](#) and the [Ethical guidelines](#) still apply. In no event shall the Royal Society of Chemistry be held responsible for any errors or omissions in this *Accepted Manuscript* or any consequences arising from the use of any information it contains.

# A Rational Design of Carbon-Supported Dispersive Pt-Based Octahedra as Efficient Oxygen Reduction Reaction Catalysts

*Xiaoqing Huang,<sup>†#</sup> Zipeng Zhao,<sup>†#</sup> Yu Chen,<sup>†</sup> Enbo Zhu,<sup>†</sup> Mufan Li,<sup>‡</sup> Xiangfeng Duan,<sup>‡§</sup>  
and Yu Huang<sup>\*†§</sup>*

<sup>†</sup>Department of Materials Science and Engineering, University of California, Los Angeles, California 90095, United States

<sup>‡</sup>Department of Chemistry and Biochemistry, University of California, Los Angeles, California 90095, United States

<sup>§</sup>California NanoSystems Institute, University of California, Los Angeles, California 90095, United States

<sup>#</sup>Xiaoqing Huang and Zipeng Zhao contributed equally to this work

<sup>\*</sup>To whom correspondence should be addressed. E-mail: [yhuang@seas.ucla.edu](mailto:yhuang@seas.ucla.edu)

**ABSTRACT:** Bimetallic PtNi nanocrystals represent an emerging class of newly discovered electrocatalysts which are expected to exhibit exciting oxygen reduction reaction (ORR) activity. Colloidal syntheses have been proven to be suitable for controlling PtNi nanocrystals with well-defined morphologies and tunable compositions with the use of capping agents or ligands. However, these colloidal PtNi nanocrystals have inherent limitations associated with the ligand-covered surfaces, which not only limits the free access of surface active sites but also hinders electron transport between the catalyst and the support, leading to deteriorated ORR performance. Herein, we report a facile one-pot strategy to synthesize highly dispersive PtNi octahedra directly on various carbon materials without using any bulky capping agents, which enhances the surface exposure of the PtNi octahedra and their catalytic activity over ORR while largely reduces the preparation costs. The obtained octahedral PtNi/C catalysts have a high ORR activity of  $2.53 \text{ mA/cm}^2$  and  $1.62 \text{ A/mg}_{\text{Pt}}$  at  $0.9 \text{ V}$  versus RHE, which are far better than those of commercial Pt/C catalysts ( $0.131 \text{ mA/cm}^2$  and  $0.092 \text{ A/mg}_{\text{Pt}}$ , all the ORR measurements were performed at room temperature in  $\text{O}_2$ -purged  $0.1 \text{ M HClO}_4$  solutions at a sweep rate of  $10 \text{ mV/s}$ ). This strategy has been extended to fabricate trimetallic PtNiCo octahedrons on carbon black with a further enhanced activity up to  $3.88 \text{ mA/cm}^2$  and  $2.33 \text{ A/mg}_{\text{Pt}}$  at  $0.9 \text{ V}$  versus RHE. The octahedral PtNiCo/C catalyst is also more stable than the commercial Pt/C in the ORR condition and shows small activity change after 6000 potential sweeps. The work demonstrates that the carbon-supported Pt-based materials reported herein are promising material candidates with enhanced performances for practical electrocatalytic applications.

**TEXT:** Fuel cells are a promising type of energy conversion device which can be potentially developed for future transportation vehicles and portable electronic

devices.<sup>[1-4]</sup> A fuel cell catalyzes reactions between the fuel (hydrogen, alcohols, etc.) at the anode and the oxidant (molecular oxygen) at the cathode, converting chemical energy of the fuel into electrical power.<sup>[5-7]</sup> Both the fuel oxidation reaction at the anode and the oxygen reduction reaction (ORR) at the cathode require catalysts to lower their electrochemical over potentials and obtain a high voltage output. Platinum (Pt) has been the universal catalyst for both reactions due to its high activity.<sup>[8,9]</sup> However, the promise of its practical application is largely hindered by the high cost of Pt in the catalysts and the slow kinetics of ORR at cathode.<sup>[10-12]</sup>

Towards developing enhanced ORR catalysts, significant advances have been made to the syntheses of Pt-based nanocrystals with precise control over size, shape, composition and structure by colloidal synthetic methods.<sup>[13-24]</sup> As a common feature, colloidal syntheses involve bulky capping agents, such as surfactants, polymers, and ionic or fatty ligands, which are necessary to stabilize and to prevent aggregations of nanocrystals during synthesis. However, the presence of the bulky capping agents on the surface of the nanocrystals will restrict the free access of O<sub>2</sub> to the surface of nanocrystals, leading to the undesirable decrease in ORR activity.<sup>[25,26]</sup> While post growth ligand removal can render a cleaner surface, it usually involves thermal and oxidative treatments that will inevitably affect the size or morphology of the particles, which in-turn alters their ORR activity.<sup>[27]</sup> In addition, in practice these ORR catalysts are usually supported on commercially available carbon black with high surface area, aiming to maximize the conductivity and dispersity of the pre-synthesized Pt-based nanocrystals.<sup>[25-26, 28]</sup> These two-step preparation, i.e. catalysts syntheses and the following dispersion on supports, however, are neither cost-effective nor efficient.<sup>[25-26]</sup> Moreover, the remaining bulky surface ligand may hinder electron transport between

the catalyst and the support, further reducing its performance. Therefore, it is highly desirable to develop effective strategies and innovative approaches for preparing highly efficient electrocatalysts with a reduced content of Pt, a more freely accessible surface and an efficient preparation method while exhibiting superior performance.

We now report a highly efficient strategy that allows the one-pot preparation of highly dispersive Pt-based octahedra on various carbon materials without using any bulky capping agents, which enhances the surface exposure of the octahedra and in turn their catalytic activity over ORR, while largely reduces the preparation costs. Our work presents several unique features: 1) we show an efficient one-pot synthetic strategy that produces dispersive PtNi octahedra on carbon black directly, which simplifies the catalyst preparation steps; 2) The octahedral PtNi nanocrystals are synthesized without using any bulky capping agents, which enhances the surface exposure of the PtNi octahedra and their catalytic activity over ORR. The resulting octahedral PtNi/C is a high-performing electrocatalyst ( $2.53 \text{ mA/cm}^2$  and  $1.62 \text{ A/mg}_{\text{Pt}}$  at  $0.9 \text{ V}$  versus RHE ), demonstrating far better ORR catalytic activity over the commercially available Pt/C catalysts (Alfa Aesar, 20 wt% Pt,  $0.131 \text{ mA/cm}^2$  and  $0.092 \text{ A/mg}_{\text{Pt}}$ , all the ORR measurements were performed at room temperature in  $\text{O}_2$ -purged  $0.1 \text{ M HClO}_4$  solutions at a sweep rate of  $10 \text{ mV/s}$ ); 3) We further show that our strategy can be readily extended to fabricate trimetallic PtNiCo octahedra on carbon black with an impressive activity up to  $3.88 \text{ mA/cm}^2$  and  $2.33 \text{ A/mg}_{\text{Pt}}$  at  $0.9 \text{ V}$  versus RHE. The results demonstrate that these Pt-based octahedra prepared directly on carbon support are indeed promising candidates for practical electrocatalytic applications with a more simplified preparation scheme and greatly a enhanced performance. This demonstration of the preparation of trimetallic Pt-based catalysts

without using any bulky surfactant was not determined in previous papers.<sup>[25,26]</sup> The results reported herein suggest that to achieve the full potential of a superior catalyst, a clean interface with the support and a freely accessible surface is of significance in addition to engineering the structure and composition of the nanocrystals.

The octahedral PtNi/C catalysts were prepared by simultaneous reduction of platinum(II) acetylacetonate ( $[\text{Pt}(\text{acac})_2]$ ) and nickel(II) acetylacetonate ( $[\text{Ni}(\text{acac})_2]$ ) by using N, N-dimethylformamide (DMF) as both the solvent and reducing agent, which contained benzoic acid as the structure-directing agent and a desired support [i.e. carbon black (C), carbon nanotube (CNT), graphene oxide (GO)]. In a typical synthesis of octahedral PtNi/C catalysts,  $\text{Pt}(\text{acac})_2$ ,  $\text{Ni}(\text{acac})_2$ , benzoic acid, carbon black dispersed in DMF were added into a vial (see Supporting Information for details). After the vial had been capped, the mixture was ultrasonicated for around 5 min. The resulting homogeneous mixture was then heated at 160 °C for 12 h in an oil bath, before it was cooled to room temperature. The resulting colloidal products were collected by centrifugation and washed several times with ethanol.

The morphologies of the prepared octahedral PtNi/C catalyst were initially determined by transmission electron microscopy (TEM) (Figure 1a, Fig.S1). It is clearly revealed that highly dispersive nanocrystals are grown on the carbon black. Those nanocrystals are octahedral in shape and uniform in size, averaging  $4.2 \pm 0.4$  nm in edge length with slightly truncated corners. Considering that the relatively high temperature (160° C) and weak structure-directing agent (benzoic agent) are used in the synthesis, it is reasonable that the reaction tends to produce more thermodynamically favored slightly truncated octahedra. The highly dispersive feature is clearly presented in the high-angle annular dark-field scanning TEM (HAADF-STEM)

image (Figure 1b). The crystal structure of the obtained nanocrystals was analyzed by powder X-ray diffraction (PXRD). The PXRD pattern of the colloidal products displays typical peaks are in agreement with those of the previous reports, and can be indexed as those of face-centered cubic (fcc) Pt<sub>3</sub>Ni (Figure S1).<sup>[29,30]</sup> No detectable impurity peaks of pure Pt and/or pure Ni are observed in the PXRD pattern, indicating that only a single PtNi phase exists in the sample. The Pt/Ni composition is 72/28, as confirmed by inductively coupled plasma atomic emission spectroscopy (ICP-AES) and TEM energy-dispersive X-ray spectroscopy (TEM-EDS) (Figure S1). We further characterized the obtained nanocrystals by high-resolution TEM (HRTEM). A HRTEM image taken from an individual octahedron indicates that it is a single crystal with well-defined fringes (Fig. 1c). The lattice spacing along the edge of the octahedron is 0.22 nm, consistent with the (111) lattice spacing of the fcc Pt<sub>3</sub>Ni, confirming that the PtNi octahedra are bounded by the (111) planes. Figure 1d shows the compositional line scanning profiles across an octahedron obtained by HAADF-STEM-EDS, where Pt and Ni elements are both distributed throughout the nanocrystal.

To achieve a better understanding and control over the preparation of octahedral PtNi/C, control experiments were performed. In the synthesis, the use of benzoic acid is critical for the growth of PtNi octahedra on carbon black. The reaction in the absence of benzoic acid cannot yield PtNi octahedra (Figure S2). When benzoic acid is substituted with phenol or benzaldehyde, only small cubic, cuboctahedral or irregular particles are grown on carbon black (Figure S3), showing the important role of benzoic acid in the formation of octahedral PtNi nanocrystals in our synthesis. This might originate from the binding of benzoic acid on the (111) surface during growth.<sup>[17]</sup> The control experiment on the growth of pure Pt nanostructures reveals that pure Pt octahedra can be readily

prepared using the same approach (Figure S4), showing the versatility of the synthetic method. In the synthesis, the addition of the carbon support is critical for the growth of highly dispersive PtNi octahedra. Although the reaction in the absence of carbon support can still produce PtNi octahedra, those PtNi octahedra aggregate severely (Figure S5). We also investigated the influence of the Pt/Ni precursor ratios on the morphology and composition of the products. Figure 2a-b and Figure S6 in the Supporting Information show typical TEM images of the products prepared by simple variation of the molar ratios of the Pt and Ni precursors supplied in the synthesis, but under the same synthetic procedure. We can see that highly dispersive PtNi octahedra on carbon black are obtained in all cases. The PXRD patterns of all the nanocrystals display typical peaks, which are similar and can be indexed as fcc Pt<sub>3</sub>Ni (Figure S6). ICP-AES and TEM-EDS were used to characterize the composition of the obtained nanocrystals fully. On the basis of the ICP-AES and TEM-EDS analysis, Pt<sub>76</sub>Ni<sub>24</sub>, Pt<sub>72</sub>Ni<sub>28</sub>, and Pt<sub>71</sub>Ni<sub>29</sub> are obtained when the mole ratios of Pt(acac)<sub>2</sub>/Ni(acac)<sub>2</sub> are 3/1, 3/2 and 3/3, respectively. It is apparent that the feeding ratios of the Pt and Ni precursors have very limited or little influence on the compositions or the morphology of the PtNi nanocrystals. This may be attributed to the difficulty in reducing Ni(II)/Ni in current system and the strong tendency of Ni to alloy with Pt.<sup>[23,31]</sup> Our one-pot strategy for the preparation of carbon-supported PtNi octahedra catalysts is versatile and can be readily extended to other carbon supports, such as carbon nanotube (CNT) and reduced graphene oxide (rGO) (see Supporting Information for detailed synthetic protocols). It is found that highly dispersive PtNi octahedra could be readily grown on both CNT and rGO (Figure 2c, d), which are all active towards the ORR (Figure S7).

Furthermore, our strategy can also be extended to the synthesis of trimetallic PtNiCo octahedra on C. The synthetic protocols (see Supporting Information for details) for the preparation of trimetallic PtNiCo/C is similar to that of PtNi/C except for the introduction of additional  $\text{Co}(\text{acac})_2$  into the reaction solution. As revealed by the TEM images (Figure 3a, Figure S8), dispersive PtNiCo nanocrystals with octahedral shape are obtained, all sharing uniform size. The edge length of the octahedra is averaged at 4.4 nm. To further identify the PtNiCo/C, we also used a number of tools to analyze the structures and determine the chemical composition: (1) the lattice spacing along the edge of an octahedron shown in the HRTEM image is 0.22 nm (Figure 3b), close to that of the (111) plane of  $\text{Pt}_3\text{Ni}$  alloy (0.22 nm). (2) The ICP-AES and TEM-EDS results suggest that the molar ratio between Pt, Ni and Co is 71:25:4 (Figure 3c). (3) As shown in the compositional line profiles cross an individual octahedron (Figure 3d), Pt, Ni and Co are distributed evenly in the nanocrystal. These results clearly indicate the successful formation of (111)-terminated PtNiCo octahedra on carbon black.

Inspired by the attractive properties (highly dispersive, well-defined, and pristine) of the octahedral PtNi/C and PtNiCo/C, we initially assessed these catalysts towards the oxygen reduction reaction (ORR). Cyclic voltammetry (CV) was used to evaluate the electrochemically active surface area (EASA) of the octahedral PtNi/C and PtNiCo/C. The EASA can provide important information regarding the number of available active sites, with a higher EASA indicating that more electrochemical active sites exist. Commercial Pt/C (Figure S9A) catalyst was used as a reference for comparison. Because of the surfactant-free PtNi and PtNiCo surface, stable CVs of our catalyst could be easily achieved in several cycles. The surfactant-free PtNi octahedra shows enhanced EASA when compared with that of PtNi octahedra anchored with PVP

(Poly(vinyl pyrrolidone)) (Figure S10), confirming the better surface accessibility of our synthesized PtNi/C octahedra. Figure 4a compares the CV curves on these different catalysts recorded in N<sub>2</sub>-purged perchloric acid solution at a sweep rate of 100 mV/s. The current responses from hydrogen adsorption/desorption processes appear in the potential range of 0.05-0.35 V. The EASA is calculated by measuring the charge collected in the hydrogen adsorption/desorption region after double-layer correction and assuming a value of 210 mC/cm<sup>2</sup> for the adsorption of a hydrogen monolayer. The octahedral PtNi/C and PtNiCo/C catalysts display high EASA of 64.4 m<sup>2</sup>/g and 61.6 m<sup>2</sup>/g, respectively, which is slightly lower but comparable to that of the commercial Pt/C (77.8 m<sup>2</sup>/g, Pt particle size: 2-5 nm) catalyst.

We then evaluated the electrocatalytic performance of the octahedral PtNi/C for ORR. The ORR measurements were performed in O<sub>2</sub>-saturated 0.1 M HClO<sub>4</sub> solutions by using a glassy carbon rotating disk electrode (RDE) at room temperature with a sweep rate of 10 mV/s. Figure 4b shows the ORR polarization curves for different catalysts. We can see that the polarization curves display two distinguishable potential regions: the diffusion-limiting current region below 0.6 V and the mixed kinetic-diffusion control region between 0.6 and 1.1 V. We calculated the kinetic currents from the ORR polarization curves by considering the mass-transport correction according to the Levich–Koutecky equation:  $1/i = 1/i_k + 1/i_d$  (where  $i_k$  is the kinetic current and  $i_d$  is the diffusion-limiting current).<sup>[32,33]</sup> In order to compare the activity for different catalysts, the kinetic currents were normalized with respect to both EASA and the loading amount of metal Pt. As shown in Figure 4c, the octahedral PtNi/C exhibits a mass activity of 1.62 A/mg<sub>Pt</sub> on the basis of the mass of Pt at 0.9 V versus a reversible hydrogen electrode (RHE), which is 17.6 times greater than that of the Pt/C catalyst (0.092 A/mg<sub>Pt</sub>) (Figure

4c). Figure 4d shows the specific activity (i.e., kinetic current per unit surface area of catalyst) of these different catalysts. The specific activities of the aforementioned catalysts also show similar trends to that of the mass activities. The octahedral PtNi/C ( $2.53 \text{ mA/cm}^2$ ) has a specific activity of 19.3 times to that of the Pt/C catalyst ( $0.131 \text{ mA/cm}^2$ ). The octahedral PtNi/C also shows enhanced activities when compared with the octahedral Pt/C (Figure S11,  $1.01 \text{ mA/cm}^2$  and  $0.79 \text{ A/mg}_{\text{Pt}}$ ) with similar size and shape (Figure S4), revealing the critical role of composition in enhancing the activity of octahedral PtNi/C catalyst.

The trimetallic PtNiCo/C shows even better ORR activity. The obtained trimetallic PtNiCo/C have ORR specific activity at  $3.88 \text{ mA/cm}^2$  and mass activity at  $2.33 \text{ mA/mg}_{\text{Pt}}$  at 0.9 V (vs. RHE), which is 25-30 times to that of the Pt/C catalyst ( $0.131 \text{ mA/cm}^2$ ,  $0.092 \text{ A/mg}_{\text{Pt}}$ ), and higher than that of recent reported PtNi octahedra ( $3.14 \text{ mA/cm}^2$ ,  $1.45 \text{ A/mg}_{\text{Pt}}$ ) and some trimetallic Pt-based nanowires.<sup>[25,34,35]</sup> A comparison of the activities of PtNiCo/C and PtNi/C shows that the obtained trimetallic PtNiCo/C have improved ORR specific activity. We infer that the enhancement in ORR activity observed in the trimetallic PtNiCo/C may be attributed to the electronic effect of the second transition metal, Co, to PtNi, which was suggested to further fine-tune the d-band center of Pt, facilitating  $\text{O}_2$  adsorption, activation, and desorption.<sup>[34,35]</sup>

We also studied the electrochemical durability of the octahedral PtNiCo/C by using accelerated durability test (ADT) between 0.6 and 1.1 V (vs RHE) in  $\text{O}_2$ -saturated 0.1 M  $\text{HClO}_4$  at a scan rate of 50 mV/s. Figure 5a shows the ORR activities for the PtNiCo/C before, after 3000 and after 6000 potential cycles. The octahedral PtNiCo/C catalyst exhibits 14 mV and 24 mV shift for their half-wave potential after 3000 potential cycles and 6000 potential cycles. As a comparison, the commercial Pt/C catalysts are unstable

under the same reaction conditions, and their ORR polarization curves show 36 mV negative shifts after durability tests (Figure 5b). After 6000 cycles, the mass activity of the PtNiCo/C is still as high as 1.01 A/mgPt, which is 10.9-fold higher than those of commercial Pt/C catalyst. Those electrocatalysts after durability tests were also examined by TEM. As shown in Figure S9, the size of the PtNiCo/C is still largely maintained in contrast to the Pt/C. It implies that the binding of octahedral PtNiCo nanocrystals to carbon black is strong due to our *in-situ* growth strategy. While the size of the octahedral PtNiCo nanocrystals is largely maintained, their morphologies become rounded. The change of morphology likely comes from the transition metal loss (i.e. Ni, Co) after 6000 potential cycles, as confirmed by EDX analyses (Figure S9, the Pt/Ni/Co composition changes from 71/25/4 to 83/16.5/0.5, as confirmed by TEM-EDX).<sup>[26]</sup> The further enhancement of the ORR durability of the PtNiCo octahedra can be expected by incorporating other elements, such as Au.<sup>[36]</sup> Overall, the catalytic activity and durability of the PtNiCo/C are enhanced when compared with those of the commercial Pt/C catalyst.

In conclusion, we have developed a facile strategy for the one-pot preparation of highly dispersive Pt-based octahedra directly on carbon supports (i.e. octahedral PtNi/C and octahedral PtNiCo/C) without using any bulky capping agents, which enhances the surface exposure of the octahedra and their catalytic activity towards ORR while simplifying the preparation procedure. The selective use of benzoic acid was demonstrated to be most essential for the growth of well-defined octahedra on carbon materials. The obtained octahedral PtNi/C and PtNiCo/C catalysts served as highly efficient catalysts in the ORR with much better activities than those of the commercial Pt/C catalysts. The enhanced performance towards ORR could be attributed to the

highly dispersive, well-defined, pristine features and a better interface with catalytic support derived from the unique synthetic approach. Given the impressive performance towards ORR and together with its rather efficient preparation approach, the carbon-supported Pt-based octahedra are indeed promising catalysts for electrocatalytic applications.

## ASSOCIATED CONTENT

**Supporting Information.** Experimental details and data. This material is available free of charge via the Internet at <http://pubs.rsc.org>.

## Corresponding Author

yhuang@seas.ucla.edu

## ACKNOWLEDGMENT

We acknowledge the support from ARO through Award No. 54709-MS-PCS and the ONR under Award N00014-08-1-0985. We thank Electron Imaging Center of Nanomachines at CNSI for the TEM support. Y.H. acknowledges the support from Sloan Research Fellowship. X. Huang also acknowledges Jonathan C. Shaw for revising the manuscript.

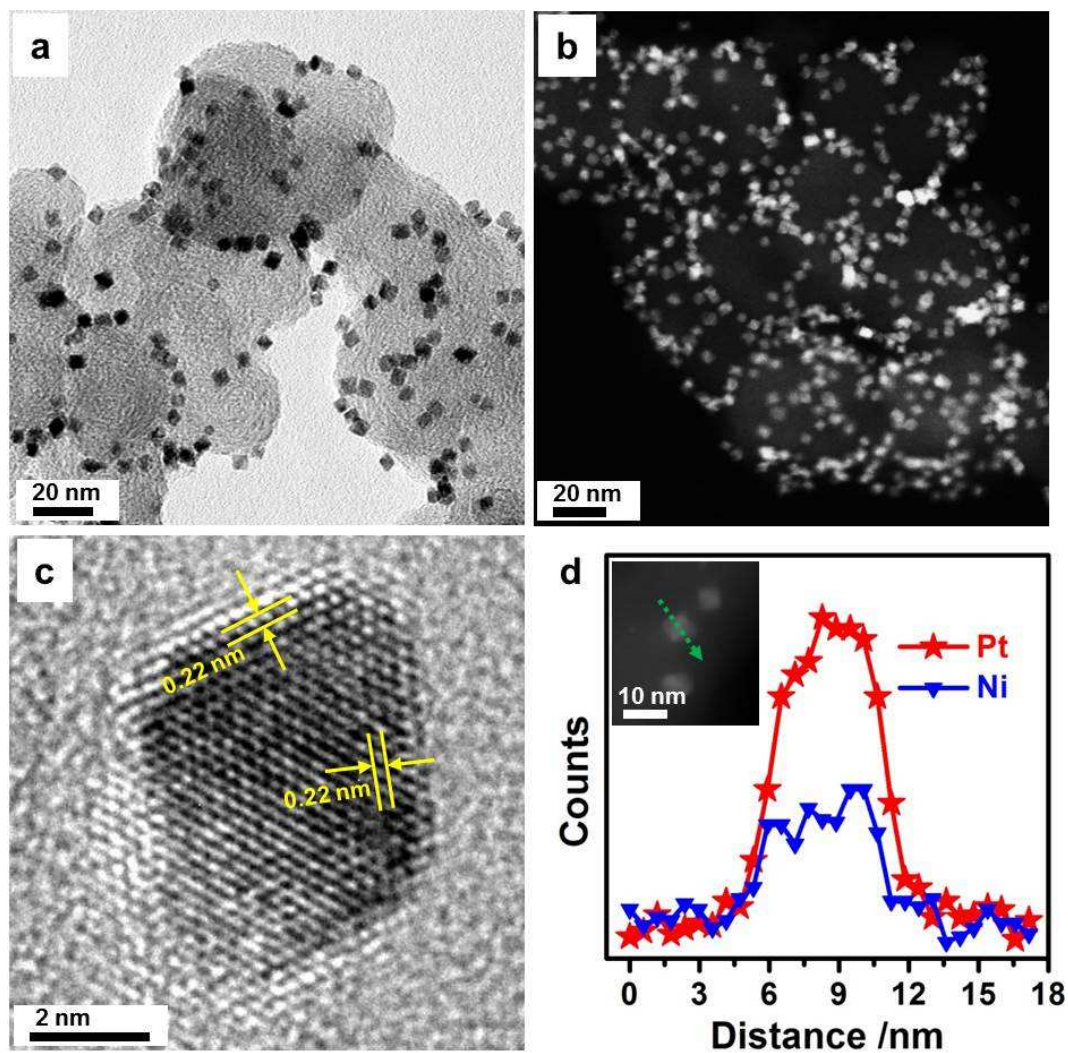
## REFERENCES:

- [1] M. Winter, R. J. Brodd, *Chem. Rev.* **2004**, 104, 4245.
- [2] Y. J. Wang, D. P. Wilkinson, J. J. Zhang, *Chem. Rev.* **2011**, 111, 7625.

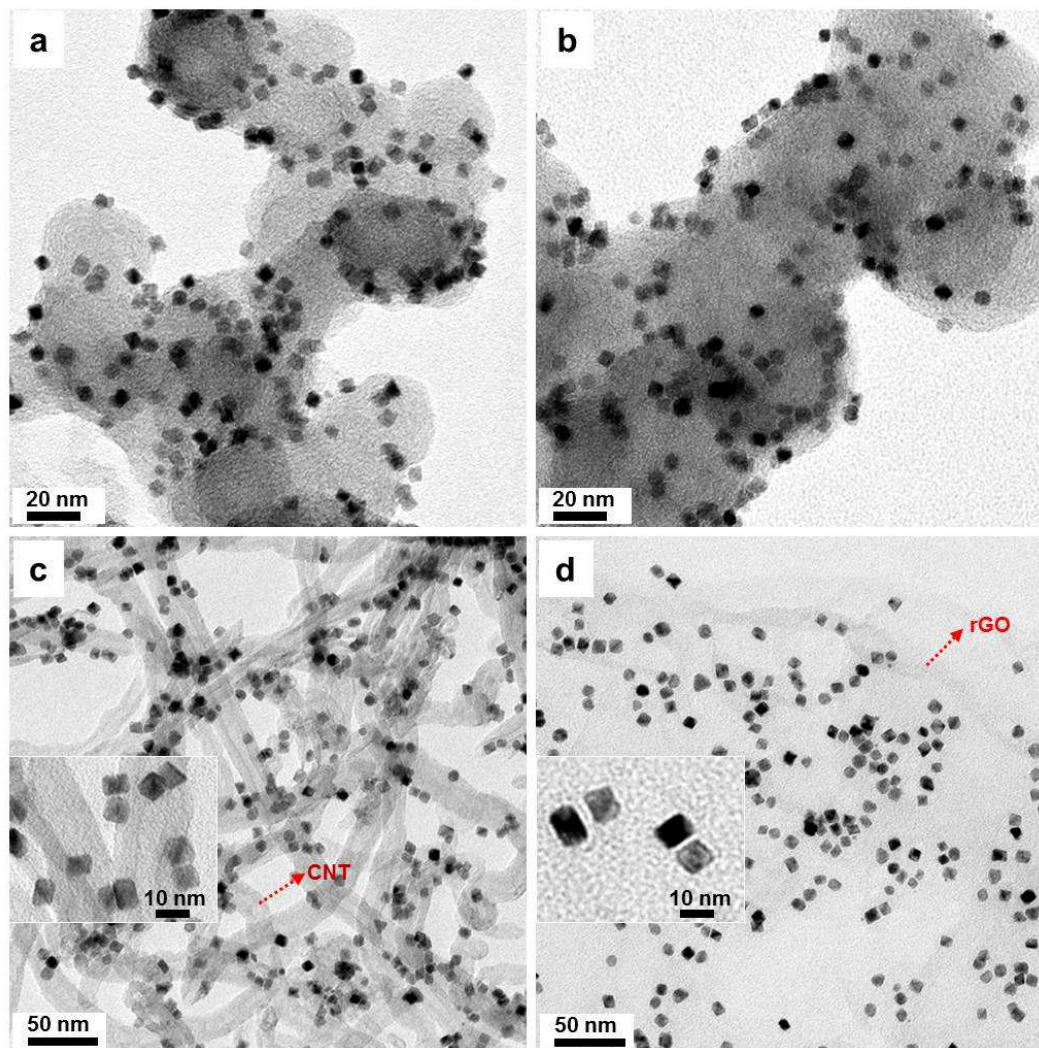
- [3] M. S. Dresselhaus, I. L. Thomas, *Nature* **2001**, 414, 332.
- [4] M. K. Debe, *Nature* **2012**, 486, 43.
- [5] Y. H. Bing, H. S. Liu, L. Zhang, D. Ghosh, J. J. Zhang, *Chem. Soc. Rev.* **2010**, 39, 2184.
- [6] D. S. Su, G. Q. Sun, *Angew. Chem., Int. Ed.* **2011**, 50, 11570.
- [7] Z. W. Chen, D. Higgins, A. P. Yu, L. Zhang, J. J. Zhang, *Energ. Environ. Sci.* **2011**, 4, 3167.
- [8] J. Y. Chen, B. Lim, E. P. Lee, Y. N. Xia, *Nano Today* **2009**, 4, 81.
- [9] N. Tian, Z. Y. Zhou, S. G. Sun, *J. Phys. Chem. C* **2008**, 112, 19801.
- [10] H. A. Gasteiger, N. M. Markovic, *Science* **2009**, 324, 48.
- [11] H. A. Gasteiger, S. S. Kocha, B. Sompalli, F. T. Wagner, *Appl. Catal., B* **2005**, 56, 9.
- [12] F. A. De Bruijn, V. A. T. Dam, G. J. M. Janssen, *Fuel Cells* **2008**, 8, 3.
- [13] J. B. Wu, A. Gross, H. Yang, *Nano. Lett.* **2011**, 11, 798.
- [14] J. Zhang, J. Y. Fang, *J. Am. Chem. Soc.* **2009**, 131, 18543.
- [15] Y. J. Kang, C. B. Murray, *J. Am. Chem. Soc.* **2010**, 132, 7568.
- [16] J. Kim, Y. Lee, S. H. Sun, *J. Am. Chem. Soc.* **2010**, 132, 4996.

- [17] Y. E. Wu, S. F. Cai, D. S. Wang, W. He, Y. D. Li, *J. Am. Chem. Soc.* **2012**, 134, 8975.
- [18] J. B. Wu, J. L. Zhang, Z. M. Peng, S. C. Yang, F. T. Wagner, H. Yang, *J. Am. Chem. Soc.* **2010**, 132, 4984.
- [19] L. Wang, Y. Nemoto, Y. Yamauchi, *J. Am. Chem. Soc.* **2011**, 133, 9674.
- [20] Z. M. Peng, H. Yang, *J. Am. Chem. Soc.* **2009**, 131, 7542.
- [21] S. I. Choi, S. F. Xie, M. H. Shao, J. H. Odell, N. Lu, H. C. Peng, L. Protsailo, S. Guerrero, J. H. Park, X. H. Xia, J. G. Wang, M. J. Kim, Y. N. Xia, *Nano Lett.* **2013**, 13, 3420.
- [22] S. J. Guo, D. G. Li, H. Y. Zhu, S. Zhang, N. M. Markovic, V. R. Stamenkovic, S. H. Sun, *Angew. Chem., Int. Ed.* **2013**, 52, 3465.
- [23] J. Zhang, H. Z. Yang, J. Y. Fang, S. Z. Zou, *Nano Lett.* **2010**, 10, 638.
- [24] X. Q. Huang, E. B. Zhu, Y. Chen, Y. J. Li, C. Y. Chiu, Y. X. Xu, Z. Y. Lin, X. F. Duan, Y. Huang, *Adv. Mater.* **2013**, 25, 2974.
- [25] C. H. Cui, L. Gan, H. H. Li, S. H. Yu, M. Heggen, P. Strasser, *Nano Lett.* **2012**, 12, 5885.
- [26] C. H. Cui, L. Gan, M. Heggen, S. Rudi, P. Strasser, *Nat. Mater.* **2013**, 12, 765.

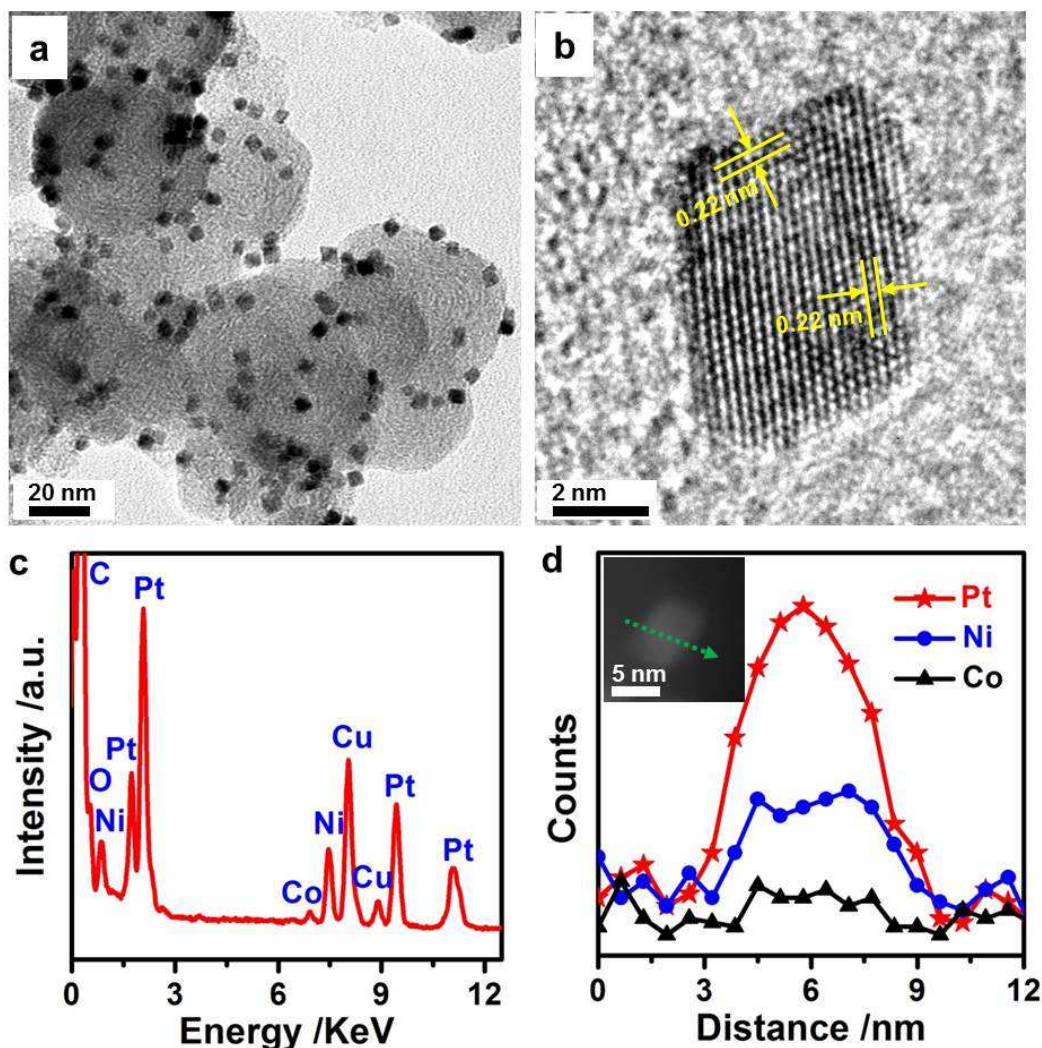
- [27] J. A. Lopez-Sanchez, N. Dimitratos, C. Hammond, G. L. Brett, L. Kesavan, S. White, P. Miedziak, R. Tiruvalam, R. L. Jenkins, A. F. Carley, D. Knight, C. J. Kiely, G. J. Hutchings, *Nat. Chem.* **2011**, 3, 551.
- [28] S. J. Guo, S. Zhang, S. H. Sun, *Angew. Chem., Int. Ed.* **2013**, 52, 8526.
- [29] K. Ahrenstorf, O. Albrecht, H. Heller, A. Kornowski, D. Gorlitz, H. Weller, *Small* **2007**, 3, 271.
- [30] K. Ahrenstorf, H. Heller, A. Kornowski, J. A. C. Broekaert, H. Weller, *Adv. Funct. Mater.* **2008**, 18, 3850.
- [31] T. C. Deivaraj, W. X. Chen, J. Y. Lee, *J. Mater. Chem.* **2003**, 13, 2555.
- [32] B. Lim, M. J. Jiang, P. H. C. Camargo, E. C. Cho, J. Tao, X. M. Lu, Y. M. Zhu, Y. N. Xia, *Science* **2009**, 324, 1302.
- [33] H. Zhang, M. S. Jin, J. G. Wang, W. Y. Li, P. H. C. Camargo, M. J. Kim, D. R. Yang, Z. X. Xie, Y. N. Xia, *J. Am. Chem. Soc.* **2011**, 133, 6078.
- [34] H. Y. Zhu, S. Zhang, S. J. Guo, D. Su, S. H. Sun, *J. Am. Chem. Soc.* **2013**, 135, 7130.
- [35] S. J. Guo, S. Zhang, D. Su, S. H. Sun, *J. Am. Chem. Soc.* **2013**, 135, 13879.
- [36] J. Zhang, K. Sasaki, E. Sutter, R. R. Adzic, *Science* **2007**, 315, 220.



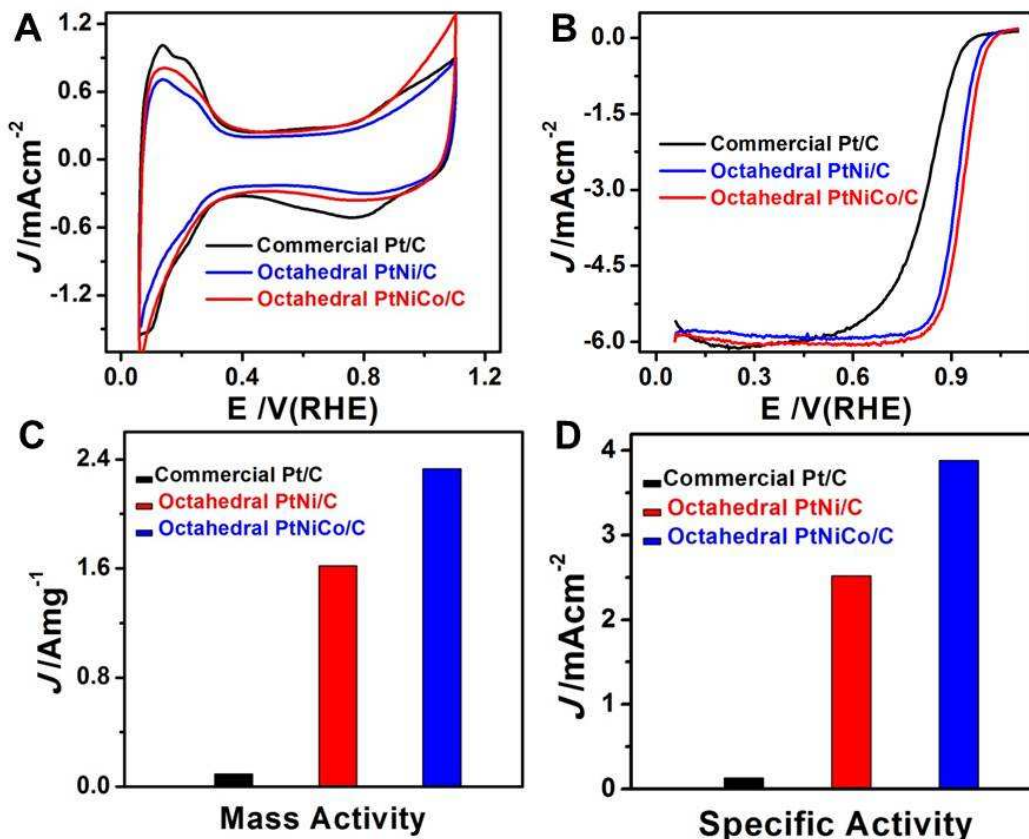
**Figure 1.** Morphology and structure analyses for octahedral PtNi/C nanocrystals. (a) Representative low-magnification TEM and (b) HAADF-STEM images of the octahedral PtNi/C nanocrystals. (c) HRTEM image on an individual octahedral PtNi/C nanocrystal. (d) Line-scanning profile across an octahedral PtNi/C nanocrystal, which is indicated in the inset of (d).



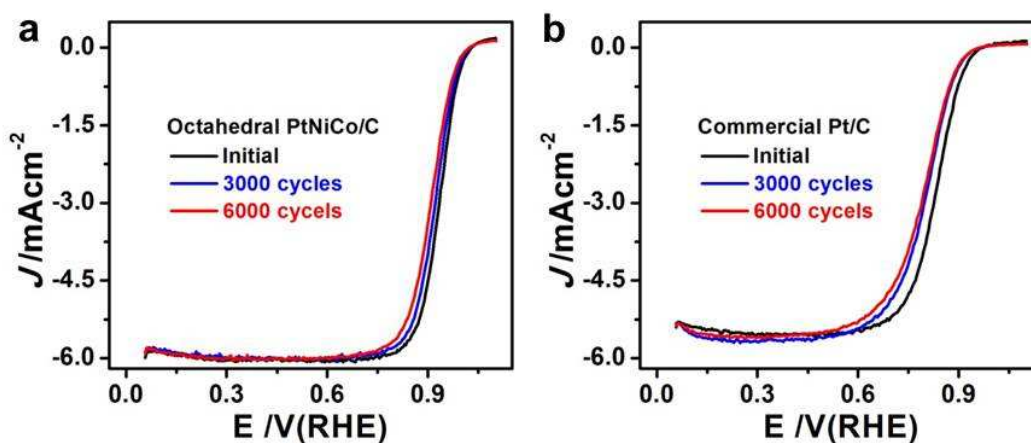
**Figure 2.** TEM images of octahedral PtNi/C nanocrystals prepared with different input molar ratio of Pt/Ni: (a) 3/1 and (b) 3/3. TEM images of octahedral PtNi grown on (c) CNT and (d) rGO. The insets in (c) and (d) show corresponding enlarged TEM images.



**Figure 3.** Morphology and structure analyses for octahedral PtNiCo/C nanocrystals. (a) Representative low-magnification TEM of the octahedral PtNiCo/C nanocrystals. (b) HRTEM image on an individual octahedral PtNiCo/C nanocrystal. (c) TEM-EDS spectra of the octahedral PtNiCo/C nanocrystals. (d) Line-scanning profile across an octahedral PtNiCo/C nanocrystal, which is indicated in the inset of (d).



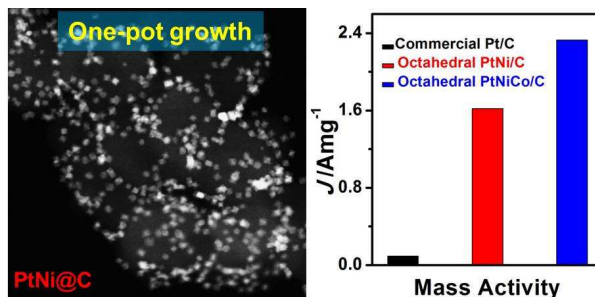
**Figure 4.** Electrocatalytic properties of octahedral PtNiCo/C catalyst, octahedral PtNi/C catalyst and Pt/C catalyst (Alfa Aesar, 20 wt% Pt). (a) Cyclic voltammograms recorded at room temperature in  $N_2$ -purged 0.1 M  $HClO_4$  solution with a sweep rate of 100 mV/s. (b) ORR polarization curves recorded at room temperature in an  $O_2$ -saturated 0.1 M  $HClO_4$  aqueous solution with a sweep rate of 10 mV/s and a rotation rate of 1600 rpm. (c, d) Mass activity and specific activity at 0.9 V versus RHE for these three catalysts, which are given as kinetic current densities normalized to the loading amount of Pt and the EASA, respectively. In (a) and (b), current densities were normalized in reference to the geometric area of the RDE ( $0.196\text{ cm}^2$ ).



**Figure 5.** Electrochemical durability of the PtNiCo/C catalyst and Pt/C catalyst. Polarization curves of (A) the octahedral PtNiCo/C catalyst (B) the commercial Pt/C catalyst before, after 3000 and after 6000 potential cycles between 0.6-1.1 V vs. RHE. The durability tests were carried out at room temperature in  $\text{O}_2$ -saturated 0.1 M  $\text{HClO}_4$  at a scan rate of 50 mV/s.

**Broader context:**

Pt based materials are widely used as catalysts in fuel cells and many heterogeneous catalytic reactions. However, because of the high cost and limited reserves of Pt, recent research efforts have focused on decreasing Pt utilization by creating advanced Pt-based catalysts. Herein, we report a facile one-pot strategy to highly dispersive PtNi octahedra on various carbon materials without using any bulky capping agents, which enhances the surface exposure of the PtNi octahedra and their catalytic activity over ORR while largely reduces the preparation costs. The obtained octahedral PtNi/C catalyst has a high ORR activity of 2.53 mA/cm<sup>2</sup> and 1.62 A/mg<sub>Pt</sub>, which are far better than those of commercial Pt/C catalysts (0.131 mA/cm<sup>2</sup> and 0.092 A/mg<sub>Pt</sub>). This strategy was also able to fabricate trimetallic PtNiCo octahedra on carbon black with a further enhanced activity up to 3.88 mA/cm<sup>2</sup> and 2.33 A/mg<sub>Pt</sub>. The octahedral PtNiCo/C catalyst is also more stable than the commercial Pt/C in the ORR condition and shows small activity change after 6000 potential sweeps. The work demonstrates that these carbon-supported Pt-based materials reported herein are indeed promising material candidates with enhanced performance for practical electrocatalytic applications.

**TOC figure:**

Highly dispersive carbon-supported octahedral Pt-based catalysts were prepared by an efficient one-pot synthetic strategy without using any bulky capping agents and were demonstrated as promising catalysts for oxygen reduction reaction (ORR).